Exciton Formation and Relaxation Dynamics in Quantum Wires

Rajesh Kumar, A. S. Vengurlekar, and A. Venu Gopal
Tata Institute of Fundamental Research, Mumbai 400005, India

T. Mélin, F. Laruelle, and B. Etienne
L2M-CNRS, 196 Avenue Henri Ravera, 92220 Bagneux, France

J. Shah
Lucent Technologies, Bell Laboratories, Holmdel, New Jersey 07733
(Received 2 June 1998)

The dynamics of one-dimensional (1D) excitons is investigated in a GaAs/AlAs quantum wire array (QWR-A) using picosecond time resolved photoluminescence (PL) measurements. The excitation density is 4×10^4 cm^{-1}, a factor of 20 below the Mott density. The rise and decay time constants of the excitonic PL in the QWR-A are 55 and 450 psec, respectively. The exciton formation time in 1D is determined to be $\approx$30 psec. Our results suggest that exciton-acoustic-phonon scattering is enhanced in 1D. However, the rates of exciton scattering with carriers and excitons is reduced. [S0031-9007(98)07167-1]

PACS numbers: 78.66.–w, 71.35.–y, 78.47.+p

Dynamics of excitons in quasi-2D systems has been extensively investigated in the past [1]. Further confinement to quasi-1D is expected to lead to significant modifications in the rates of excitonic dynamical processes, such as exciton formation, exciton scattering with carriers, excitons and phonons, and exciton relaxation and cooling. Much of the previous work on quantum wires (QWRs) is devoted to the study of carrier capture and hot carrier relaxation in QWRs at high excitation densities [2]. Experimental investigations of exciton dynamics in QWRs are relatively few and are mainly concerned with exciton recombination lifetime in QWRs [3], deduced with a time resolution of a few tens of picoseconds.

In this paper, we report the first investigation of exciton formation and relaxation dynamics in 1D systems. We perform picosecond time resolved (TR) frequency up-conversion photoluminescence (PL) measurements (at 8 K) on a AlAs/GaAs quantum wire array (QWR-A), also termed as a lateral superlattice (LSL), with a very low disorder. To compare these with 2D, we perform similar measurements on a $Al_{0.075}Ga_{0.925}As/Al_{0.33}Ga_{0.67}As$ reference quantum well (QW) in the form of a highly tilted part of the LSL with essentially no lateral band gap modulation (LBGM). Since the Al content in the reference QW is nearly the same as the average Al content of 8.5 percent in the QWR-A, any effects due to alloy disorder on exciton dynamics are similar in the two cases [4]. The QWR-A, along with the reference QW, is molecular-beam epitaxy grown on a (100) GaAs substrate, misoriented by 0.5° towards [110]. The growth sequence is shown in Fig. 1. The excited carrier density is 4×10^4 cm^{-1}, well below the Mott density ($\approx 8 \times 10^5$ cm^{-1} for 1D [5]). The PL spectra in 1D at such low excitation densities are excitonic [6]. We find that the rise of the lowest energy exciton PL is faster in the QWR-A than in the reference QW, but the exciton PL decay is slower in the QWR-A. Using the time dependence of the homogeneous linewidth of the 1D excitonic PL, we deduce the time constant for formation of 1D excitons to be $\approx$30 psec. The exciton relaxation and cooling time is estimated to be about 25 psec. Our studies indicate reduced exciton scattering with carriers and excitons but enhanced exciton-acoustic-phonon scattering compared to 2D.

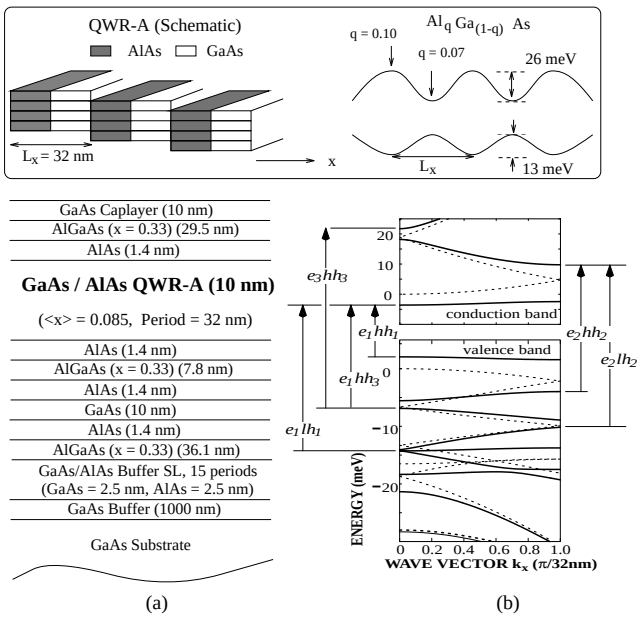

FIG. 1. The QWR-A layer structure (a) and the energy dispersion (b) for various minibands in the k_x ($k_y = 0$) direction (solid lines) are shown, along with various optical transitions possible in the absorption spectrum of the QWR-A. Also shown is the energy dispersion in the absence of lateral modulation (dotted curves). The upper panel shows a QWR-A cross section and the modulation potential schematically.

 0031-9007/98/81(12)/2578(4)$15.00

The various optical transitions in our QWR-A (Fig. 1) were studied in detail earlier by comparing the calculated and measured absorption coefficient and its linear and circular polarization ratios [8]. The transitions are labeled as e_{im}-hh_{in} or e_{im}-lh_{in}, where "m" and "n" denote mth and nth lateral minibands, resulting from the LBGM in the x direction, with a lateral superlattice period L_x. This opens minigaps at $k_x = \pm p\pi/L_x, k_y = 0$ for $p = 1, 2, \ldots$. The index i refers to quantization in the growth (z) direction. For our purpose, $i = 1$, corresponding to the first conduction subband and to the first two valence subbands. The index i therefore is not displayed in Fig. 1 and in what follows. The minibands e_1, hh_1, and lh_1 are essentially dispersionless, with insignificant wire-to-wire tunneling. The excitons associated with these minibands are one dimensional. These are seen prominently in the photoluminescence excitation (PLE) spectra of the QWR-A but signal due to e_1-hh_1 continuum is not evident. The e_1-hh_3 transition, although forbidden in 2D, is optically active in the LSL, and can be seen in the PLE spectrum.

The continuous wave (cw) PL energy spectrum obtained at 8 K shows peaks at 1.6507 and 1.6633 eV due to the lowest energy excitons in the reference QW and the QWR-A, respectively. The Gaussian full width at half maximum (FWHM) is about 4.6 meV for the QW PL peak and 6.0 meV for the QWR-A. The energy integrated cw PL for the QWR-A is nearly the same as that for the QW. The PLE Stokes shift is about 2 meV. The exciton $1s$-$2s$ splitting is $\approx$10 meV in the 2 K cw PL spectrum for the QWR-A, giving an exciton binding energy of about 12 meV. While the cw PL excitation spectrum for the QW is unpolarized, that for the QWR-A shows a polarization anisotropy, with a linear polarization ratio (LPR) of -10 percent and $+37$ percent for the e_1-hh_1 and e_1-hh_3 excitons, respectively, where LPR $= (I_x - I_y)/(I_x + I_y)$. $I_{x(y)}$ is the PLE intensity with incident light polarized perpendicular (parallel) to the wire axis (y). These observations confirm the high quality of growth and of the lateral interfaces.

Our time resolved PL measurements are performed by exciting the sample with psec pulses from a dicyanomethylene dye laser (pumped by a Nd-YAG laser) at a photon wavelength of 640 nm, below the energy of the band gap of the AlGaAs barriers of the QWR-A and the reference QW in the growth direction. The time and energy resolution is about 3.0 ps and 4.0 meV, respectively. Figure 2(a) shows the psec TR PL spectra for the QWR-A, obtained at a delay of 10 psec. The spectrum is dominated by the e_1-hh_1 1D exciton. However, additional features are clearly seen on the high energy tail of the spectrum. A comparison with PLE spectra shows that they occur at energies corresponding to e_1-hh_3 and e_1-lh_1 excitons. The e_2-hh_2 exciton, about 4 meV above the e_1-lh_1 exciton, is somewhat weaker than the e_1-lh_1 exciton in the PLE spectrum. This is not well resolved in Fig. 2(a). These tail contributions, however, vanish at larger delays, as is evident from the spectrum at 100 psec

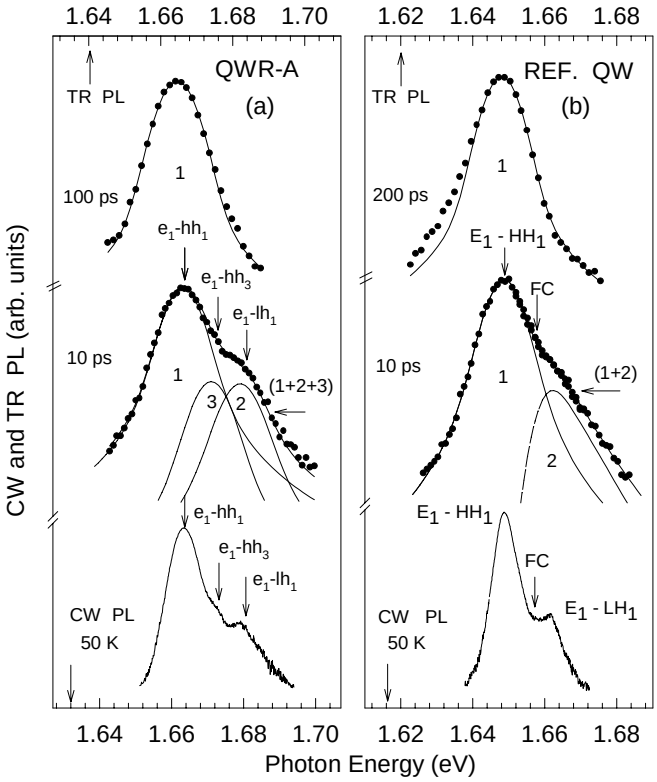

FIG. 2. The TR PL spectra at 10 psec and at a larger delay, together with cw PL spectra at 50 K are shown for the QWR-A (a) and the reference QW (b) (on semilogarithmic scale). [There is a small relative shift in the energy axes in (a).] 1, 2, and 3 in (a) and 1 in (b) refer to exciton line shape fit, and 2 in (b) to free carrier PL fit, respectively.

shown in Fig. 2(a). Although the cw PL spectrum at 8 K shows only the e_1-hh_1 exciton, we expect the e_1-hh_3 and e_1-lh_1 exciton states to get occupied as the lattice temperature increases. The cw PL at 50 K, shown in Fig. 2(a) as an example, clearly identifies the PL due to these excitons. A fit based on a simple calculation of line shapes for PL contributions arising from the above transitions satisfies the TR PL spectra very well. *The results of Fig. 2(a) provide evidence for luminescence due to excitons of zone folded minibands of the QWR-A.*

It is interesting to compare the above results in QWR-A with those obtained for the 2D reference QW [Fig. 2(b)] at identical excitation densities. As expected, the TR PL spectra for the QW are dominated by recombination of the heavy hole excitons (referred to as E_1-HH_1). The shoulder seen on the high energy side of the spectra at 10 psec is due to free e-h recombination, since it is known that the light hole related excitons (E_1-LH_1) in QWs decay rapidly (except at very low densities, $<10^9$ cm^{-1}) [9] and, hence, are not resolved in TR PL spectra, even at short delays. [The light hole exciton, however, can be seen in PLE spectrum for the QW. Also, as expected, the light hole exciton occupancy for the QW can be revealed in the cw PL spectra at elevated lattice temperatures, as in Fig. 2(b).] In contrast, the e_1-hh_3 and e_1-lh_1 excitons

for the QWR-A can be seen both in the PLE and TR PL spectra (at short delays) at low temperatures. This implies that the rate of decay of the e_1-lh_1 (and e_1-hh_3) excitons in the QWR-A, presumably via their transfer to the e_1-hh_1 continuum in the QWR-A, is much slower than that of the transfer of the light hole exciton to the E_1-HH_1 continuum in the QW. We find that the *sum of the spectrally integrated contributions due to the* e_1-lh_1 *and* e_1-hh_3 *excitonic PL,* deduced from the line shape fits described above for the QWR-A, *rises and decays with a time constant of about 5 and 40 psec, respectively.*

In Fig. 3, we show the time evolution of luminescence due to the lowest energy excitons (e_1-hh_1 and E_1-HH_1, respectively) in the QWR-A and the reference QW, obtained at identical excitation densities. The exciton PL in the 1D is seen to rise with an exponential time constant of 55 psec. In contrast, the excitonic PL for the QW rises with a larger time constant of 85 psec.

The rise time of excitonic PL is a combined result of carrier relaxation towards the subband edges, exciton formation at large K, and the subsequent relaxation of large K excitons to $K \approx 0$, where they can couple to light [10]. It is reasonable to assume that carrier cooling and relaxation in the upper 2D-like states of the QWR-A and the QW are similar. This process may contribute a few psecs to the rise time of the exciton PL. The major part of the rise time originates from exciton formation and relaxation. Later, we show that the exciton formation time in the QWR-A and the QW is approximately 30 and 45 psec, respectively. This, together with the rise time of 55 psec for the 1D excitonic PL, leads to the exciton relaxation time of the order of 25 psec in 1D. The corresponding estimate for the QW is larger by 60 percent. Thus, the faster exciton PL rise for the QWR-A in Fig. 3 is mainly a result of faster exciton relaxation in 1D. This suggests that *the strength of exciton-acoustic-phonon scattering, which primarily determines exciton relaxation at low densities, is enhanced in 1D.* This is consistent with the enhancement indicated earlier in measurements of temperature dependent exciton dephasing rates in four wave mixing (FWM) experiments [11,12] on QWR-A.

The 1D exciton PL in Fig. 3 has a decay time of about 450 psec, larger than the decay time of 320 psec for the QW exciton. That the decay is mainly radiative is indicated by the weak temperature dependence for the PL peak intensities below 50 K observed in our cw PL spectral measurements on both the QWR-A and the reference QW. The *intrinsic* radiative lifetime of 1D excitons at $K \approx 0$ is expected to be an order of magnitude larger than in 2D due to reduced exciton spatial coherence in 1D [13]. However, experimentally measured exciton PL decay times are thermally averaged radiative lifetimes (τ_r). Since the thermal population of excitons at $K > 0$ in 2D is larger than in 1D, τ_r in 1D is larger than in 2D only by $\eta = 3.83/\sqrt{T}$, as found in the experiments of Akiyama *et al.* [3] on their QWRs and QWs. ($\eta \approx 1.35$ for $T = 8$ K, close to the value of 1.4 obtained here.)

It is possible to estimate the 1D exciton formation time from the time dependence of the homogeneous linewidth of the e_1-hh_1 1D excitonic PL as follows. The TR PL spectra, corrected for instrument response, may be fitted by a convolution of a Lorentzian (for homogeneous broadening) and a Gaussian (for inhomogeneous broadening) [14] using a procedure described in detail elsewhere [10,15,16]. This excitonic line shape satisfies the PL spectra very well for most of the delay values. Small deviations appear on the high energy tails at delays smaller than 100 psec or so, as seen in Fig. 2(a) and are due to e_1-lh_1 and e_1-hh_3 excitons. In Fig. 4, we show the homogeneous FWHM (Γ_L) obtained using the above procedure. It has been suggested

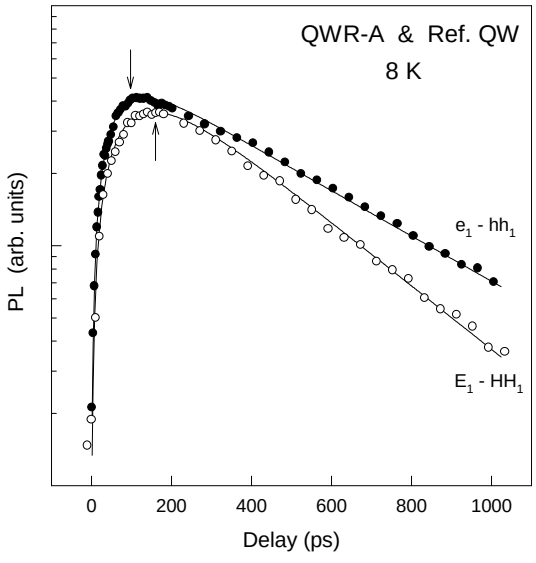

FIG. 3. The time dependence of PL for the QWR-A and the reference QW at energies corresponding to e_1-hh_1 and E_1-HH_1 exciton PL peaks, respectively (see Fig. 2) is shown, along with exponential fits (solid lines). Arrows indicate delays at which the TR PLs reach maxima.

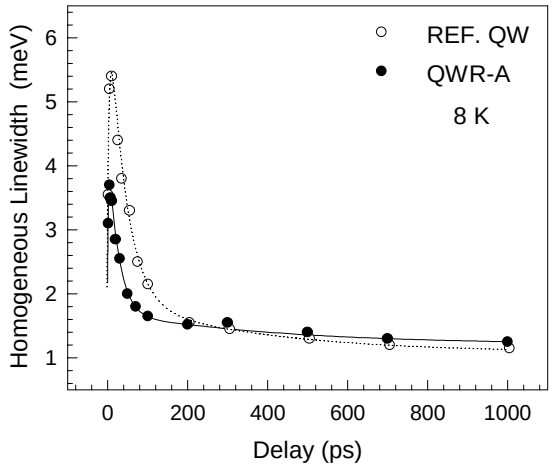

FIG. 4. The time evolution of the homogeneous linewidth for exciton PL for QWR-A and reference QW is shown along with theoretical fits.

that free carrier-exciton scattering is the dominant cause for exciton line broadening in QWs in the early stages of exciton time evolution. The rapid initial decay of Γ_L in Fig. 4 is mainly related to the decay of carrier density due to exciton formation, as in 2D [10]. To further analyze the data of Fig. 4, we write, in analogy with the 2D case [17]: $\Gamma_L(t) = \Gamma_0 + a_{1D}E_B[\gamma_{xc}n_c(t) + \gamma_{xx}n_x(t)]$, where a_{1D} and E_B are the 1D exciton Bohr radius and binding energy, respectively. The coefficient γ_{xc} (γ_{xx}) represents the effect of exciton scattering with carriers (excitons) on Γ_L. The densities of free carriers $[n_c(t)]$ and excitons $[n_x(t)]$ may be obtained by solving a simple model of exciton formation [16,18] using coupled rate equations for n_c, n_d (large K exciton density), and n_r ($K \approx 0$ exciton density), expressed in terms of exponential time constants, τ_0 and τ_1 for the rise and decay of n_c, and τ_d and τ_r for the decay of n_d (due to large K exciton relaxation to $K \approx 0$) and n_r, respectively. Also, n_x ($= n_d + n_r$) is the total exciton density. A very satisfactory fit to Γ_L of Fig. 4, and the time evolution of the energy integrated exciton PL intensity is obtained, giving us estimates of the time constants. We find that $n_c(t)$ decays rapidly in about 100 psec, approximately with a time constant $\tau_1 = 30$ psec. *This determines the time constant for formation of 1D excitons in our QWR-A to be about 30 psec.* In comparison, a similar analysis for the 2D case using our PL measurements on the reference QW leads to an exciton formation time of ≈45 psec. As in QWs, the 1D excitons are also presumably formed at $K > 0$. The somewhat smaller τ_1 in 1D, in spite of reduced density of states for 1D excitons at large K, may be a result of enhanced exciton-acoustic-phonon scattering. The 1D exciton relaxation time (τ_d) is found to be ≈30 psec, close to the estimate of 25 psec, made earlier. This may be compared with $\tau_d \approx 45$ psec, deduced for the reference QW, implying slower relaxation.

The coefficients γ_{xc} and γ_{xx}, indicating the strengths of carrier-exciton and exciton-exciton scattering in 1D, are found to be 6.9 and 1.0, respectively, using $a_{1D} = 9$ nm and $E_B = 12$ meV. These are smaller than the corresponding values of 11.8 and 1.4 deduced for our reference QW using $a_{1D} = 10$ nm and $E_B = 9$ meV. This shows that *exciton-carrier and exciton-exciton scattering is weaker in 1D*. Presumably, this is a consequence of the restrictions of phase space and energy-momentum conservation in electron-exciton scattering in 1D. Previously, reduced exciton-exciton scattering was also inferred by Oestreich *et al.* [19] from TR PL measurements on etch-patterned QWRs with an active wire width of 60 nm. It may be mentioned that the values of the scattering coefficients γ_{xc} and γ_{xx} deduced above for the $Al_{0.075}Ga_{0.925}As$ reference QW are nearly the same as those obtained in TR PL experiments on 8 nm GaAs QWs [20]. Previously, $\gamma_{xc} = 11.5$ and $\gamma_{xx} = 1.5$ were obtained for the 2D case in FWM experiments [17] on 12 nm GaAs QWs.

In summary, we have obtained the first information on dynamics of 1D excitons in a quantum wire array using picosecond time resolved PL measurements at low temperatures and low excitation densities. We find that the 1D excitonic luminescence rises and decays with time constants of 55 and 450 psec, respectively. We deduce the exciton formation and relaxation times to be 30 and 25 psec, respectively. Our results suggest that exciton-acoustic-phonon scattering is enhanced in 1D. However, the exciton scattering with carriers and excitons is weaker than in 2D. Our measurements also reveal the presence of excitonic luminescence associated with zone folded minibands of the QWR-A.

Partial support for this work to A. S. V., F. L., and B. E. by the IFCPAR under Grant No. 1514-1 and to A. S. V. and J. S. by NSF under Grants No. INT-9714915 and No. INT-9702021 is gratefully acknowledged.

[1] J. Shah, *Ultrafast Spectroscopy of Semiconductors and Nanostructures* (Springer-Verlag, Berlin, 1996).
[2] R. Cingolani *et al.,* Phys. Rev. Lett. **67**, 891 (1991); A. C. Maciel *et al.,* Appl. Phys. Lett. **66**, 3039 (1995); J. F. Ryan *et al.,* Phys. Rev. B **53**, 4225 (1996); R. Ambigapathy *et al.,* Phys. Rev. Lett. **78**, 3579 (1997).
[3] H. Akiyama *et al.,* Phys. Rev. Lett. **72**, 924 (1994); D. Gershoni *et al.,* Phys. Rev. B **50**, 8930 (1994); M. S. Miller *et al.,* Phys. Rev. Lett. **68**, 3464 (1992).
[4] Since alloy scattering can cause only momentum relaxation, it does not affect the exciton formation and energy relaxation rates directly. However, possible enhancement in exciton-phonon interactions due to alloy disorder may increase these rates, and, hence, may somewhat reduce exciton PL rise time.
[5] F. Rossi and E. Molinari, Phys. Rev. Lett. **76**, 3642 (1996).
[6] Unlike the case of 2D, e-h Coulomb correlation in 1D is expected to suppress the oscillator strength for optical transitions of e-h pairs in the 1D continuum for low density excitations, with the Sommerfeld factor vanishing at the subband edge [5,7].
[7] T. Ogawa and T. Takagahara, Phys. Rev. B **43**, 14 325 (1991).
[8] J. Bloch, U. Bockelmann, and F. Laruelle, Europhys. Lett. **28**, 501 (1994); B. Etienne *et al.,* J. Cryst. Growth **150**, 336 (1995); T. Mélin and F. Laruelle (to be published).
[9] Ph. Roussignol *et al.,* Phys. Rev. B **45**, 6965 (1992); R. Eccleston *et al.,* Phys. Rev. B **44**, 1395 (1991).
[10] T. C. Damen *et al.,* Phys. Rev. B **42**, 7434 (1990).
[11] E. J. Mayer *et al.,* Phys. Rev. B **49**, 2993 (1994).
[12] W. Braun *et al.,* Phys. Rev. B **56**, 12 096 (1997).
[13] D. Citrin, Phys. Rev. Lett. **69**, 3393 (1992).
[14] Y. Chen, G. P. Kothiyal, J. Singh, and P. K. Bhattacharya, Superlattices Microstruct. **3**, 657 (1987); J. Christen and D. Bimberg, Phys. Rev. B **42**, 7213 (1990).
[15] D. Robart *et al.,* Solid State Commun. **95**, 287 (1995).
[16] R. Kumar *et al.,* Phys. Rev. B **54**, 4891 (1996); R. Kumar *et al.,* J. Appl. Phys. **80**, 5921 (1996).
[17] A. Honold, L. Schultheis, J. Kuhl, and C. W. Tu, Phys. Rev. B **40**, 6442 (1989).
[18] J. Kusano *et al.,* Phys. Rev. B **40**, 1685 (1989).
[19] M. Oestreich *et al.,* Phys. Rev. Lett. **70**, 1682 (1993).
[20] Rajesh Kumar, Ph.D. thesis, University of Mumbai, 1998.